Gastric Cancer (2023) 26:691–707
https://doi.org/10.1007/s10120-023-01405-1

ORIGINAL ARTICLE

Gastric cancer mesenchymal stem cells via the CXCR2/HK2/PD-L1 pathway mediate immunosuppression

Chao Huang[1] · Bin Chen[1,6] · Xin Wang[2] · Juan Xu[3] · Li Sun[1,7] · Deqiang Wang[4] · Yuanyuan Zhao[1] · Chenglin Zhou[3] · Qiuzhi Gao[1] · Qianqian Wang[1] · Zhihong Chen[5] · Mei Wang[1] · Xu Zhang[1] · Wenrong Xu[1] · Bo Shen[2] · Wei Zhu[1]

Received: 10 March 2023 / Accepted: 25 May 2023 / Published online: 10 June 2023

Abstract

Background Anti-PD-1 immunotherapy has emerged as an important therapeutic modality in advanced gastric cancer (GC). However, drug resistance frequently develops, limiting its effectiveness.

Methods The role of gastric cancer mesenchymal stem cells (GCMSCs) in anti-PD-1 resistance was evaluated in vivo in NPG^{CD34+} or NCG^{PBMC} xenograft mouse model. In addition, we investigated $CD8^+$T cell infiltration and effector function by spectral cytometry and IHC. The effects of GCMSCs conditional medium (GCMSC-CM) on GC cell lines were characterized at the level of the proteome, secretome using western blot, and ELISA assays.

Results We reported that GCMSCs mediated tolerance mechanisms contribute to tumor immunotherapy tolerance. GCMSC-CM attenuated the antitumor activity of PD-1 antibody and inhibited immune response in humanized mouse model. In GC cells under serum deprivation and hypoxia, GCMSC-CM promoted GC cells proliferation via upregulating PD-L1 expression. Mechanistically, GCMSC-derived IL-8 and AKT-mediated phosphorylation facilitated HK2 nuclear localization. Phosphorylated-HK2 promoted PD-L1 transcription by binding to HIF-1α. What is more, GCMSC-CM also induced lactate overproduction in GC cells in vitro and xenograft tumors in vivo, leading to impaired function of $CD8^+$ T cells. Furthermore, CXCR1/2 receptor depletion, CXCR2 receptor antagonist AZD5069 and IL-8 neutralizing antibody application also significantly reversed GCMSCs mediated immunosuppression, restoring the antitumor capacity of PD-1 antibody.

Conclusions Our findings reveal that blocking GCMSCs-derived IL-8/CXCR2 pathway decreasing PD-L1 expression and lactate production, improving antitumor efficacy of anti-PD-1 immunotherapy, may be of value for the treatment of advanced gastric carcinoma.

Chao Huang and Bin Chen contributed equally to this work.

Bo Shen and Wei Zhu jointly supervised this work.

✉ Wei Zhu
zhuwei@ujs.edu.cn

[1] School of Medicine, Jiangsu University, 301 Xuefu Road, Jingkou District, Zhenjiang, Jiangsu, China

[2] Department of Oncology, Jiangsu Cancer Hospital and Jiangsu Institute of Cancer Research and, The Affiliated Cancer Hospital of Nanjing Medical University, Nanjing, Jiangsu, China

[3] Department of Laboratory Medicine, Affiliated Taizhou People's Hospital of Nanjing Medical University, Taizhou, Jiangsu, China

[4] Department of Oncology, Affiliated Hospital of Jiangsu University, Zhenjiang, Jiangsu, China

[5] Department of Gastrointestinal Surgery, Affiliated People's Hospital of Jiangsu University, Zhenjiang, Jiangsu, China

[6] Department of Clinical Laboratory, Affiliated Hospital of Jining Medical University, Jining, Shandong, China

[7] Department of Clinical Laboratory, Kunshan First People′s Hospital, Kunshan, China

Graphical abstract

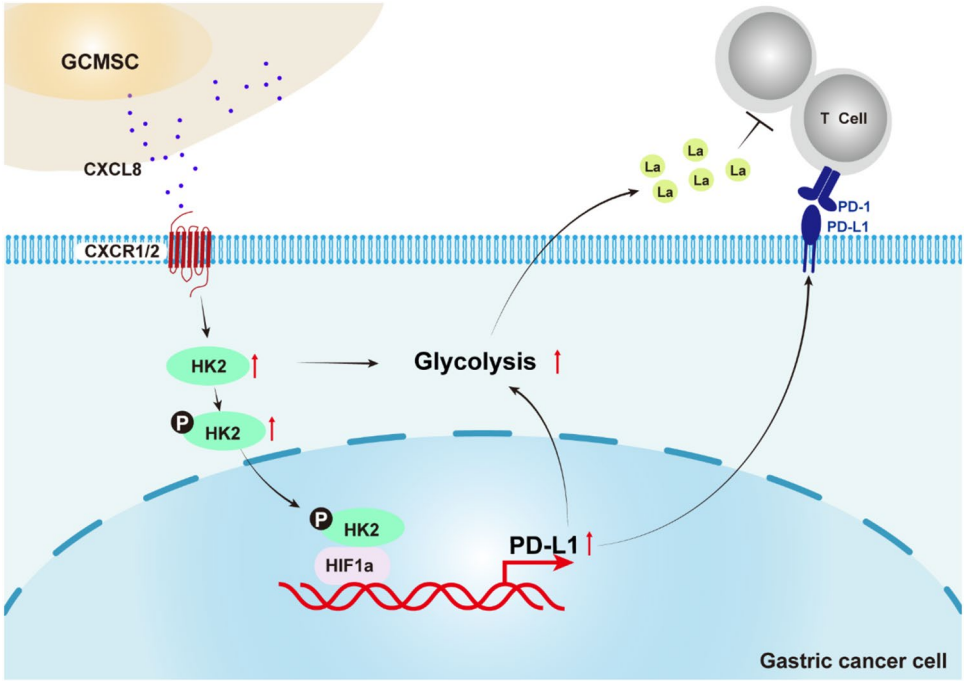

Keywords Gastric cancer mesenchymal stem cells · Anti-PD-1 · HK2 · IL-8 · CXCR2

Abbreviations

TME	Tumor microenvironment
PD-1	Programmed death-1
PD-L1	Programmed death ligand-1
HK2	Hexokinase II
PBMCs	Peripheral blood mononuclear cells
MSCs	Mesenchymal stem cells
GCMSCs	Gastric cancer mesenchymal stem cells
BMMSCs	Bone marrow mesenchymal stem cells
HIF-1α	Hypoxia-inducible factor-1α
CXCR1	C-X-C motif chemokine receptor 1
CXCR2	C-X-C motif chemokine receptor 2
IL-8	Interleukin-8
IL-1	Interleukin-1
IFN-γ	Interferon γ

Background

Due to its frequently advanced stage at diagnosis, advanced gastric cancer lacks an effective treatment, making its mortality high. Tumor immune checkpoint blockade (ICB) has brought new hope to patients and achieved a breakthrough in the research field or clinical practice. However, the objective response rate (ORR) of advanced GC immunotherapy was less than 30% in patients treated with a single agent, such as nivolumab or pembrolizumab [1–3], indicating the existence of unexplored mechanisms of immunosuppressive microenvironment in GC, which leads to evasion of ICB. Delineating the exact mechanisms of tumor immune control and evasion enables the development of novel and highly effective therapies.

IL-8 regulates inflammatory responses by binding to CXC chemokine receptor 1 (CXCR1) and CXC chemokine receptor 2 (CXCR2) receptors [4]. Accumulating evidences have shown that IL-8 promotes tumor growth and metastasis through multiple mechanisms, such as inhibiting antitumor cytotoxic T cell functions, promoting angiogenesis, and forming neutrophil extracellular traps [5–8]. Clinical trial results have indicated that elevated serum and intratumoral IL-8 levels were negatively associated with the clinical efficacy of anti-PD-1 therapy [9, 10]. Notably, GCMSCs secreted IL-8 was greater than marrow mesenchymal stem cells (BMMSCs) in vitro, which significantly elevated expression levels of programmed death ligand 1 (PD-L1) in GC [11]. Here, we show that blocking the GCMSC-derived IL-8/CXCR2/HK2 signal pathway could improve antitumor immunity and suppress tumor growth in GC.

Methods

Patients and sample collection

Fresh resected GC tumor samples were put on ice and taken within 2 h to the laboratory to start dissection and processing from Affiliated People's Hospital of Jiangsu University (Zhenjiang, Jiangsu, China). Patients with autoimmune disease, infectious diseases, or multi-primary cancers were not included. The clinical stages of tumors were determined according to the tumor, node, metastases (TNM) classification system of the international union against cancer. GCMSCs were isolated from human GC tissues as previously described [12]. Briefly, fresh GC tissues were cut into approximately 1 mm^3-sized pieces. Adherent culture was maintained until the mensenchymal-like cells reached 85% confluence, and the cells were trypsinized and expanded for up to five passages.

A total of 39 patients (29 males and 10 females) with unresectable gastric cancer were recruited from the Affiliated Cancer Hospital of Nanjing Medical University (Nanjing, Jiangsu, China) or the Affiliated Hospital of Jiangsu University (Zhenjiang, Jiangsu, China) to investigate the association between IL-8 serum levels and the efficacy of PD-1 antibody treatment. These patients received anti-PD-1-based immunotherapy combined with chemotherapy, and their clinical characteristics are summarized in Supplementary Data Table 1. Tumors were assessed via computed tomography or magnetic resonance imaging (per Response Evaluation Criteria in Solid Tumors (RECIST), version 1.1).

To explore the association between intratumoral lactate levels and the expression of HK2, IFN-γ, and granzyme B (GZMB), 18 patients who underwent gastric resections for GC were recruited from the Affiliated Hospital of Jiangsu University. The GC tissue samples were collected during gastric resection. The clinical characteristics of the patients are summarized in Supplementary Data Table 2. The inclusion and exclusion criteria are shown in the material.

All patients signed informed consent forms, and this study was approved by the Ethics Committee of the Affiliated Cancer Hospital of Nanjing Medical University and the Affiliated Hospital of Jiangsu University.

Cell culture

GCMSCs were isolated and maintained in α-MEM supplemented with 10% fetal bovine serum (FBS) at 37 °C in a humidified atmosphere of 5% CO_2, as previously described [13]. Human peripheral blood mononuclear cells (PBMCs) were isolated and maintained in RPMI 1640 supplemented with 10% FBS at 37 °C in a humidified atmosphere of 5% CO_2, as previously described [14]. Human gastric cancer cell lines MGC-803, HGC-27, and SGC-7901 were purchased from the Cell Bank of Type Culture Collection of Chinese Academy of Sciences (Beijing, China) and maintained in RPMI 1640 supplemented with 10% FBS at 37 °C in a humidified atmosphere of 5% CO_2. To prepare the conditioned medium (CM), GCMSCs or BMMSCs at 80% confluency were washed with phosphate-buffered saline (PBS) and incubated with fresh α-MEM supplemented with 10% FBS for 48 h. Then, the culture medium was collected, filtered through a 0.22 μm filter, and diluted with RPMI 1640 containing 10% FBS at a ratio of 1:1. To account for patient heterogeneity, we blended multiple batches of supernatant to ensure a consistent effect.

$CD34^+$ humanized mouse model

To establish a $CD34^+$ humanized mouse model, male NOD-*Prkdc*^{scid} *Il2rg*^{tm1}/Vst (NPG) mice (Stock No.: VS-AM001) aged 4 ~ 8-week-old were purchased from Beijing Vitalstar Biotechnology (Beijing, China). Human $CD34^+$ cells were isolated from human umbilical cord blood and stored in liquid nitrogen until transplantation. NPG mice were irradiated by X-ray (1.2 Gy), and 5×10^4 human $CD34^+$ cells were transplanted intravenously into each mouse within 24 h after irradiation. At 12 weeks after transplantation, flow cytometry was performed to determine the proportion of human $CD45^+$ cells in the peripheral blood. Mice with over 25% $hCD45^+$ cells in peripheral blood were considered $CD34^+$ humanized mice (NPG^{CD34+}).

Humanized PBMC mouse model

To establish humanized PBMC mouse models, male NOD/ShiLtJGpt-*Prkdc*^{em26Cd52}*Il2rg*^{em26Cd22}/Gpt (NCG) mice aged 4 ~ 8-week-old were purchased from Nanjing GemPharmatech (Nanjing, Jiangsu, China). Human PBMCs were collected from the peripheral blood of volunteers. Each NCG mouse was transplanted with 1×10^7 human PBMCs intraperitoneally. At 7 days after transplantation, flow cytometry was performed to determine the proportion of human $CD45^+$ cells in the peripheral blood. Mice with over 25% $hCD45^+$ cells in peripheral blood were considered humanized PBMC mice (NCG^{PBMC}).

Flow cytometry

For mouse tumor tissue samples, a single-cell suspension was obtained by treating samples with 1 mg/mL collagenase (#C9263, Sigma), 2 U/mL Dispase II (#04942078001, Roche), 0.1 mg/mL DNase (#DN25,

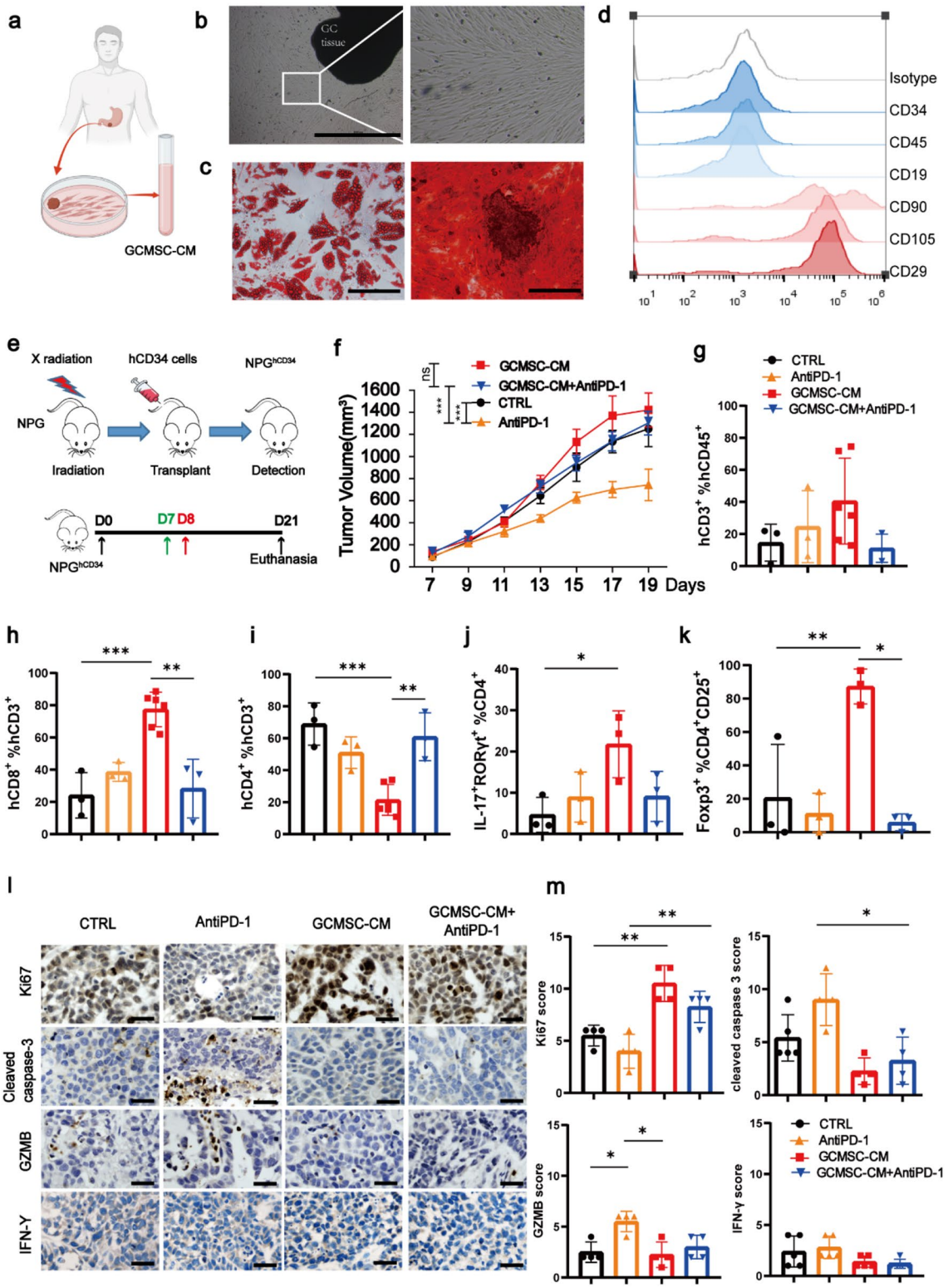

Sigma), 1 mg/mL Hyaluronidase (#H8030, Solarbio). To perform surface antigens staining, tissue lysates or cells were incubated with FITC mouse anti-human CD8 (1:50; #555,366; BD Biosciences, San Jose, CA, USA), FITC mouse anti-human CD4 (1:50; #55,346; BD Biosciences) antibody at 4 °C for 30 min. Cells were then incubated with APC Anti-human IFN-γ (1:20; #502,512; Biolegend) antibody at 4 °C for 30 min. After washing with a permeabilization buffer (Thermo Fisher Scientific), cells

◂**Fig. 1** GCMSC attenuated the antitumor effect of PD-1 antibody on gastric tumor in mice. **a** Schematic diagram of GCMSCs isolated from GC patient-derived fresh tissues and GCMSC-CM collection. **b** GCMSCs culture bright field picture (scale bar: 2000 μm). **c** Representative images showing osteogenesis (left) and adipogenesis (right) of GCMSCs (scale bar: 50 μm). **d** Flow cytometry detected GCMSCs characteristic molecular markers. **e** Schematic diagram of SGC-7901 xenograft tumor-bearing NPG^{CD34+} mice model. "Green" arrows indicate "administered GCMSC-CM (200uL) via subcutaneous injection peritumoral", "red" arrows show "administered pembrolizumab (10 mg/kg) via intraperitoneal injection", $n=6$. **f** Growth curves of tumor-bearing NPG^{CD34+} mice. **g–k** Human $CD45^+CD3^+$, $CD3^+CD8^+$, $CD3^+CD4^+$, IL-$17^+ROR\gamma t^+CD4^+$ $Foxp3^+$ $CD4^+$ $CD45^+$ cells in tumor tissue of mice were detected by flow cytometry. **l** The expression of Ki67, cleaved caspase-3, granzyme B (GZMB), and interferon γ (IFN-γ) in tumor tissue samples from NPG^{CD34+} mice were detected by immunohistochemical (IHC) staining (scale bar: 50 μm). **m** Quantification of (**i**) data are expressed as the mean ± standard error of the mean (SEM). $^*P<0.05$, $^{**}P<0.01$, $^{***}P<0.001$

were resuspended in PBS and analyzed using a Beckman CytoFLEX analyzer (Indianapolis, IN, USA).

Western blot and phos-tag™ analyses

Proteins were separated using 10% sodium dodecyl sulfate polyacrylamide gel electrophoresis (SDS-PAGE) and then transferred to polyvinylidene fluoride (PVDF) membranes (Millipore, Billerica, MA, USA). For HK2 phosphorylation detection, total proteins were separated using 10% Mn^{2+}-phos-tag™-SDS-PAGE ($MnCl_2$ and phos-tag™ were added). Further procedures are provided in the Supplementary Data materials.

Electrophoretic mobility shift assay (EMSA)

EMSA was performed to examine the effect of HK2 on hypoxia-inducible factor 1 α (HIF-1α) transcriptional activity using a chemiluminescent EMSA Kit (GS009; Beyotime, Shanghai, China) following the manufacturer's instruction. Further procedures are provided in the Supplementary Data materials.

Immunohistochemistry (IHC) and hematoxylin–eosin (HE) staining

IHC was conducted using an IHC kit (Boster Biological Technology, Wuhan, Hubei, China) following the manufacturer's instructions. HE staining was performed using an HE staining kit (Solarbio, Beijing, China) following the manufacturer's instructions. For IHC, staining intensity was assessed as 0 (negative), 1 (weak), 2 (medium), or 3 (strong) score, while the staining extent was scored as 0 (0% of the staining area), 1 (1 ~ 25%), 2 (26 ~ 50%), 3 (51 ~ 75%), and 4 (76 ~ 100%). The IHC score was calculated by multiplying the staining intensity and extent scores. Further procedures are provided in the Supplementary Data materials.

Enzyme-linked immunosorbent assay (ELISA)

The serum IL-8 levels were determined by utilizing an ELISA kit (EK108HS-96; Multisciences, Hangzhou, Zhejiang, China) in accordance with the manufacturer's instructions. The optical density was obtained by subtracting the readings obtained at 630 nm from the readings at 450 nm. A standard curve was utilized to measure the concentrations of IL-8.

Small interfering RNA (siRNA)- and small hairpin RNA (shRNA)-mediated gene knockdown

HK2 siRNA (sense: 5′-GAGAAUCAGAUCUAUGCCATT-3'; antisense: 5′-UGGCAUAGAUCUGAUUCUCTT-3′) and negative control were purchased from RiboBio (Guangzhou, Guangdong, China). The siRNA was transfected into cells using Lipofectamine® 2000 (Invitrogen) according to the manufacturer's instructions. PD-L1 shRNA (5′-GCACAT CCTCCAAATGAAAGG-3′) and negative control were purchased from GenePharma (Shanghai, China) and transfected into cells following the manufacturer's instructions.

CRISPR/Cas9-mediated knockout of CXCR1 and CXCR2

Knockout of human CXCR1 and CXCR2 genes in HGC-27 cell was performed using CRISPR/Cas 9 gene-editing technology. The procedures are described in the Supplementary Data materials.

Statistical analysis

Data were expressed as the mean ± standard error of the meant. Statistical analysis was performed using the Prism 6 software (GraphPad, San Diego, CA, USA) or SPSS 22.0 software (Chicago, IL, USA). Differences between groups were analyzed using a student's t test or one-way analysis of variance. The Kruskal–Wallis H test was used to analyze the differences between in vivo tumor growths. $p<0.05$ was considered to be statistically significant.

Results

GCMSC-CM attenuates the antitumor effect of PD-1 antibody in NPG^{CD34+} mice

We isolated GCMSCs from fresh gastric tumor tissues and collected GCMSCs conditional medium (GCMSC-CM)

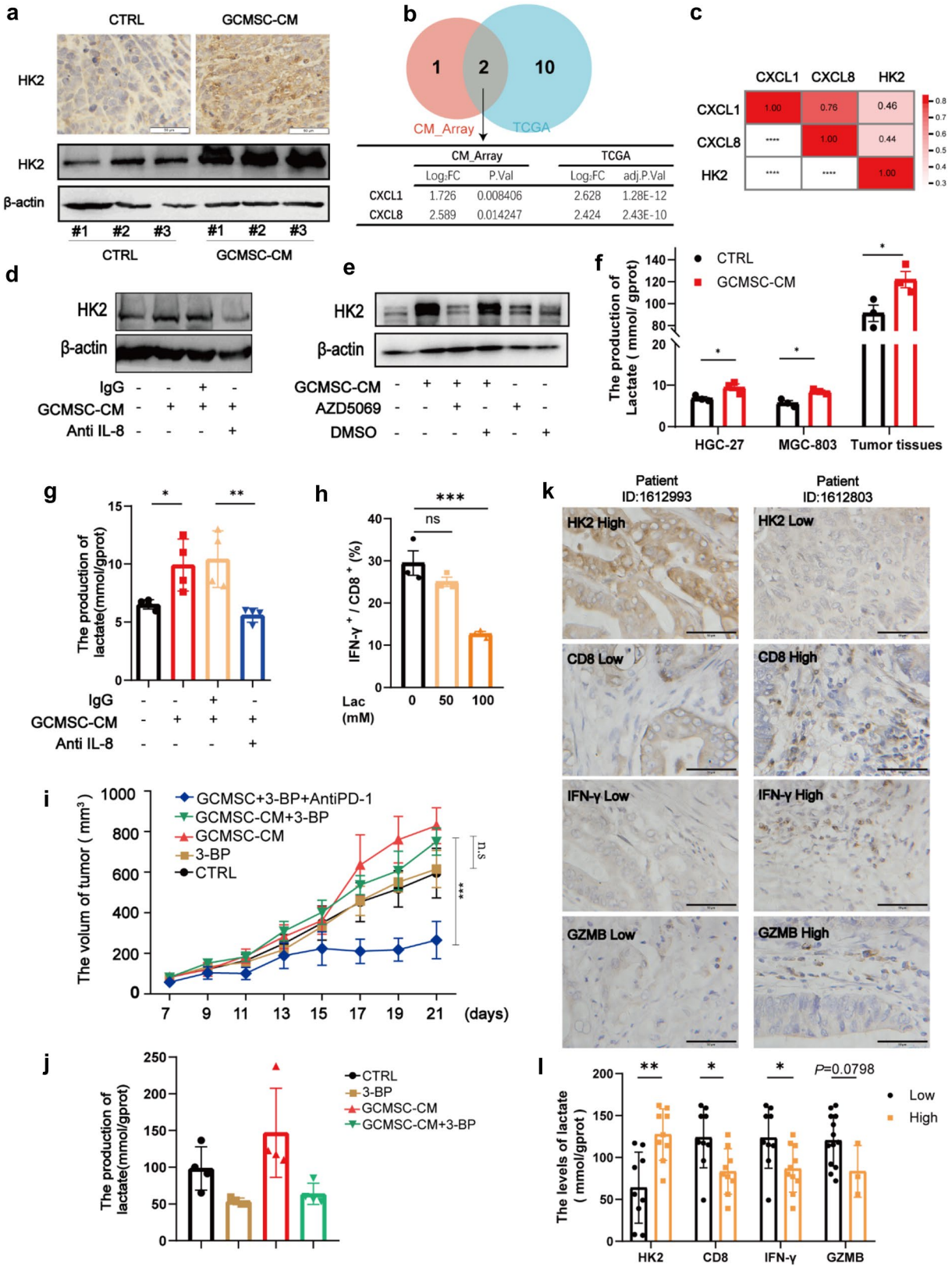
a
CTRL
GCMSC-CM
HK2
HK2
β-actin
#1 #2 #3 #1 #2 #3
CTRL
GCMSC-CM
b
1
2
10
CM_Array
TCGA
CM_Array
TCGA
Log2FC P.Val Log2FC adj.P.Val
CXCL1 1.726 0.008406 2.628 1.28E-12
CXCL8 2.589 0.014247 2.424 2.43E-10
c
CXCL1 CXCL8 HK2
CXCL1 1.00 0.76 0.46
CXCL8 **** 1.00 0.44
HK2 **** **** 1.00
d
HK2
β-actin
IgG - - + -
GCMSC-CM - + + +
Anti IL-8 - - - +
e
HK2
β-actin
GCMSC-CM - + + + - -
AZD5069 - - + - + -
DMSO - - - + - +
f
The production of Lactate (mmol/ gprot)
CTRL
GCMSC-CM
HGC-27
MGC-803
Tumor tissues
g
The production of lactate(mmol/gprot)
IgG - - + -
GCMSC-CM - + + +
Anti IL-8 - - - +
h
IFN-γ+ / CD8+ (%)
ns
Lac (mM)
0 50 100
i
The volum of tumor (mm3)
GCMSC+3-BP+AntiPD-1
GCMSC-CM+3-BP
GCMSC-CM
3-BP
CTRL
n.s
(days)
j
The production of lactate(mmol/gprot)
CTRL
3-BP
GCMSC-CM
GCMSC-CM+3-BP
k
Patient ID:1612993
Patient ID:1612803
HK2 High
HK2 Low
CD8 Low
CD8 High
IFN-γ Low
IFN-γ High
GZMB Low
GZMB High
l
The levels of lactate (mmol/gprot)
P=0.0798
Low
High
HK2 CD8 IFN-γ GZMB

◂**Fig. 2** GCMSC-CM increased lactate production in gastric cancer cells via the IL-8/HK2 pathway. **a** IHC staining and immunoblot assays for HK2 in NPG^{CD34+} mouse (scale bar: 50 μm). **b** Venn diagram according to the fold change and *P* value of GCMSC-CM Human Cytokine Array versus STAD of TCGA database. **c** Heatmap revealed a positive correlation between CXCL1, CXCL8, and HK2 in STAD. Immunoblot assays for HK2 expression. **d** Immunoblot assays in HGC-27 with GCMSC-CM or anti-IL-8 neutralizing antibody treatment. **e** Immunoblot assays in HGC-27 with GCMSC-CM or CXCR2 inhibitor AZD5069 treatment. **f** Lactate content was measured in HGC-27, MGC-803 cells, and tumor tissues treated as indicated. **g** Lactate content was measured in HGC-27 that received the indicated treatment. **h** Flow cytometry analysis was conducted to determine IFN-γ expression in $CD8^+$ T cells treated with different concentrations of lactate. **i** Growth curves of HGC-27 xenograft tumor-bearing NCG^{PBMC} mice. 3-BP (8 mg/kg) via intraperitoneal injection every 3 days. All mice were killed on day 21. **j** The lactate content was measured in tumor tissues treated as indicated. **k** Two representative patients with $HK2^{Low\backslash High}$, IHC staining for CD8, GZMB, and IFN-γ in pathological tissue sections (n = 18). **l** GC patients-derived fresh tissues lactate content was measured in patients' tissues in different groups according to IHC score of HK2, CD8, GZMB, and IFN-γ

(Fig. 1a, b), which was confirmed by Oil red O and alizarin red staining after specific differentiation induction (Fig. 1c), as well as characteristic surface molecule detection (CD90, CD105, CD29) and negative expression (CD45, CD34, CD19) of hematopoietic markers via flow cytometry (Fig. 1d). To investigate whether GCMSCs impair anti-PD-1 treatment efficacy in GC, we constructed an SGC-7901 tumor xenograft model in NPG^{CD34+} mice and treated them with GCMSC-CM and PD-1 antibody individually or in combination (Fig. 1e). At 21 days after treatment, we observed that PD-1 antibody treatment significantly suppressed gastric tumor growth, while the combination of GCMSC-CM and PD-1 antibody resulted in significantly increased tumor volumes compared to PD-1 antibody treatment alone, indicating that GCMSC-CM abrogates the inhibitory effect of PD-1 antibody on gastric tumor growth (Fig. 1f).

Additionally, we analyzed the immune cells in tumor tissue collected from NPG^{CD34+} mice tumor tissues (Fig. 1g) and PBMCs at the end of the experiment (Supplementary Data Table 3). We found that although GCMSC-CM treatment could increase effector cells $CD8^+$ $CD3^+$ cell and $IL17^+$ $ROR\gamma t^+CD4^+$ cell number (Fig. 1h, j), it failed to suppress tumor growth. Notably, we observed markedly reduced proportion of the $CD4^+$ $CD3^+$ cell subset (Fig. 1i), but elevated proportion of the $FOXP3^+$ $CD4^+$ $CD25^+$ cell subset in tumor tissue (Fig. 1k). Furthermore, we explored cell proliferation, apoptosis, and the function of immune cells in response to GCMSC-CM treatment. IHC staining showed that GCMSC-CM treatment inhibited cell apoptosis and immune response, while promoting cell proliferation, thus attenuating the inhibitory effect of PD-1 antibody on gastric tumor growth (Fig. 1l). Additionally, we observed increased collagen fiber production around the tumor tissue and a concentration of $GZMB^+$ cells in the invasive margin area in the GCMSC-CM treatment group (Supplementary Fig. S1A, B). Collectively, our results suggest that GCMSC-CM promotes cell proliferation, while inhibiting cell apoptosis and immune response in gastric tumor tissue, thereby attenuating the inhibitory effect of PD-1 antibody on gastric tumor growth.

GCMSC-CM increased lactate production in gastric cancer cells via the CXCR2/HK2 pathway

To further investigate the reasons for the insufficient infiltration of immune effector cells at the tumor location, based on our previous findings that GCMSC upregulated HK2 expression in vitro and promoted tumor growth [15], we hypothesized that GCMSC-CM treatment could have affected the HK2-mediated glycolysis in tumor cells, thereby inhibiting the antitumor immune response. We examined the level of HK2 expression in tumor tissues (Fig. 2a) and analyzed the upregulated secreted proteins in GCMSC-CM compared with BMMSC-CM using human cytokine array [11]. Venn diagram analysis identified two overlapping upgraded chemokine genes within the TCGA_STAD database, indicating that IL-1 (CXCL1) or IL-8 (CXCL8) might be the most noteworthy cytokine in glucose flux reprogramming (Fig. 2b, c). To explore the role of IL-8 in HK2 expression of GC cells, which was the most dramatic fold change within GCMSC-CM, we performed an IL-8 neutralizing antibody to pretreat GCMSC-CM to deplete GCMSC-derived IL-8, and the results demonstrated that GCMSC-CM could not increase HK2 expression in GC cells without IL-8 (Fig. 2d). Considering that CXCR2 is IL-1 and IL-8 co-receptor, CXCR2 inhibitor AZD5069 was used to inhibit receptor signaling, and we found that AZD5069 significantly decreased HK2 expression (Fig. 2e), To investigate whether the increased HK2 expression affects lactic acid production in GC cells. GCMSC-CM treatment was also found to elevated lactate production in GC cells and tumor tissue (Fig. 2f), while neutralizing IL-8 could antagonize this effect (Fig. 2g). We further discovered that lactate exposure significantly reduced IFN-γ production in $CD8^+$ T cells in a dose-dependent manner (Fig. 2h). To assess whether inhibiting HK2 activity would improve the antitumor efficacy of PD-1 antibody in vivo, we applied gastric cancer xenograft NCG^{PBMC} mice with GCMSC-CM, PD-1 antibody Keytruda, and HK2 inhibitor 3-BP individually or in combination (Fig. 2i). The results showed that 3-BP alone failed to suppress tumor growth in mice, whereas cotreatment with PD-1 antibody and 3-BP considerably reduced the volumes of tumors even in the presence of GCMSC-CM. We further found that 3-BP treatment effectively inhibited GCMSC-CM-induced overproduction of lactate in xenograft

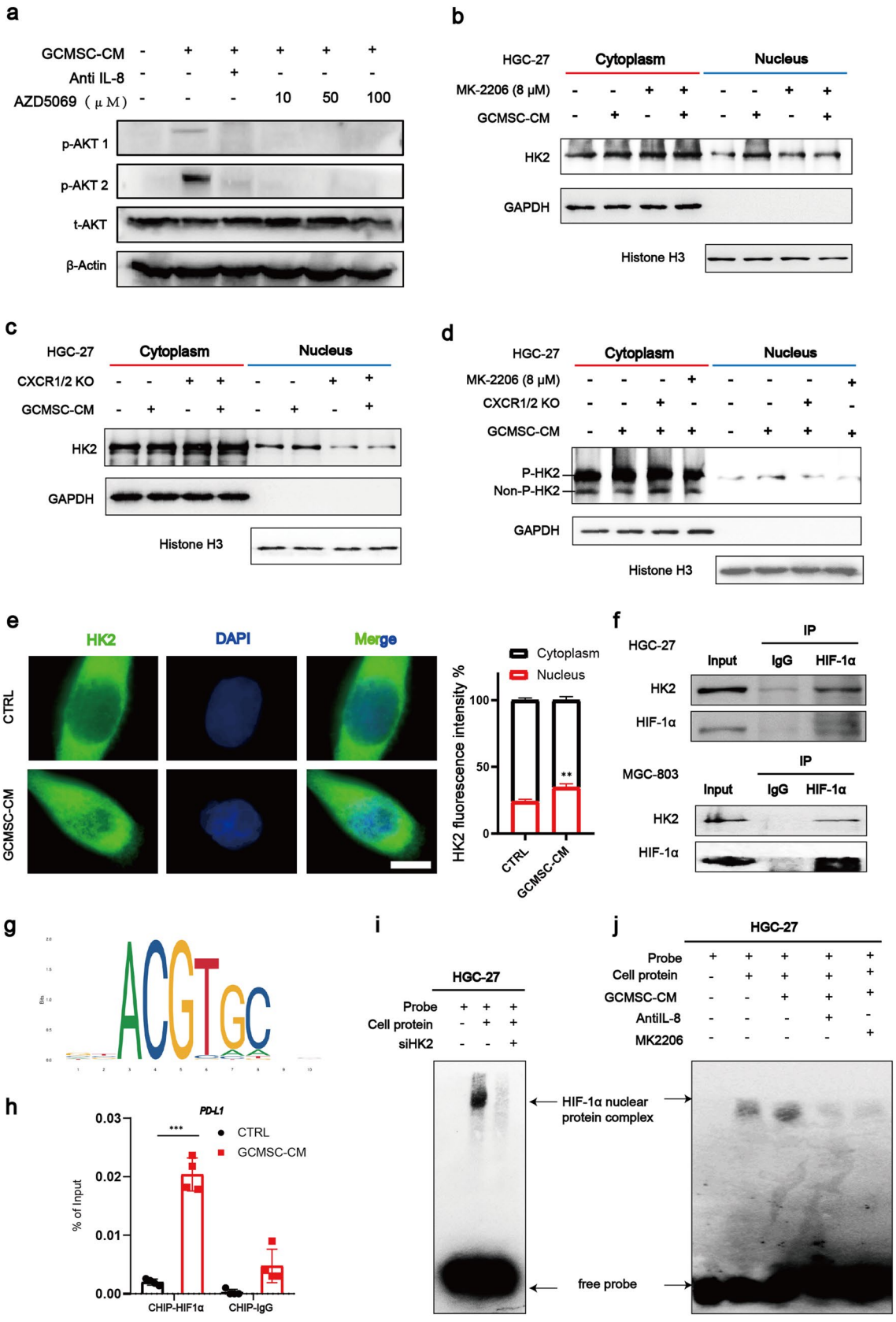
a
GCMSC-CM
Anti IL-8
AZD5069 (μM)
p-AKT 1
p-AKT 2
t-AKT
β-Actin
b
HGC-27
Cytoplasm
Nucleus
MK-2206 (8 μM)
GCMSC-CM
HK2
GAPDH
Histone H3
c
HGC-27
Cytoplasm
Nucleus
CXCR1/2 KO
GCMSC-CM
HK2
GAPDH
Histone H3
d
HGC-27
Cytoplasm
Nucleus
MK-2206 (8 μM)
CXCR1/2 KO
GCMSC-CM
P-HK2
Non-P-HK2
GAPDH
Histone H3
e
HK2
DAPI
Merge
CTRL
GCMSC-CM
HK2 fluorescence intensity %
Cytoplasm
Nucleus
f
HGC-27
IP
Input
IgG
HIF-1α
HK2
HIF-1α
MGC-803
g
h
PD-L1
% of Input
CTRL
GCMSC-CM
CHIP-HIF1α
CHIP-IgG
i
HGC-27
Probe
Cell protein
siHK2
HIF-1α nuclear protein complex
free probe
j
HGC-27
Probe
Cell protein
GCMSC-CM
AntiIL-8
MK2206

◂**Fig. 3** Phosphorylation is required for HK2 nuclear localization to regulate PD-L1 transcription. **a** Immunoblot assays was performed to determine AKT phosphorylation of HGC-27 with indicated treatment 1 h. **b**, **c** Immunoblot assays were performed to determine HK2 protein expression in the cytoplasm or nucleus of HGC-27 wild-type or CXCR1 and CXCR2 receptor knocked out by CRISPR–Cas9 for 6 h. **d** SDS-PAGE$^{Phos-tag}$ analysis was conducted to determine HK2 phosphorylation in HGC-27 cells treated as indicated 6 h. **e** Immunofluorescence assay was performed to verify the nuclear/cytoplasmic expression ratio of HK2 protein for GCMSC-CM treated for 6 h. **f** Co-IP was conducted to examine HK2/HIF-1α interaction in HGC-27 and MGC-803 cells for 12 h. **g** Sequence logo of HIF-1α-binding motif in the hPD-L1 promoter region. **h** Occupation frequency of HIF-1α on the gene region of hPD-L1 was detected by ChIP-qPCR assays for 12 h. **i**, **j** Electrophoretic mobility shift assay was carried out to examine HIF-1α transcriptional activity in HGC-27 cells, HK2-silenced or treated with IL-8 neutralizing antibody or MK2206 for 12 h

tumor tissue (Fig. 2j). We observed that lactate concentration was significantly increased in human GC tissue samples ($N=18$) with a high HK2 expression group, but decreased in those with high CD8, GZMB, and IFN-γ expression groups (Fig. 2k, l). Collectively, those data suggested that HK2-mediated lactate production inhibited the antitumor effect of anti-PD-1 in the presence of GCMSC-CM.

Phosphorylation is required for HK2 nuclear localization to regulate PD-L1 transcription

To further explore the mechanism by which GCMSC-derived IL-8 weakens the efficacy of anti-PD-1 through the IL-8/CXCR2/HK2 pathway, a microarray of SGC-7901 cells was carried out to identify the transcriptional alterations after BMMSC-CM or GCMSC-CM treatment. Pathway analysis revealed that the Class I PI3K/AKT signal pathway was positively enriched in the GCMSC-CM group compared with the control group treated with BMMSC-CM (Supplementary Fig. S2A). What is more, according to HK2 protein sequencing, amino acid site T473 may be phosphorylated by AKT signaling (Supplementary Fig. S2B). Immunoblot assay demonstrated that GCMSC-CM-induced AKT phosphorylation was inhibited by AZD5069 (Fig. 3a). In our previous study, we found that GCMSC-derived IL-8 was capable of upregulating PD-L1 expression in GC cells [11]. Therefore, we hypothesized that IL-8/AKT mediates HK2 nuclear localization and phosphorylation to promote PD-L1 expression in GC cells. We found that GCMSC-CM increased the nuclear expression of HK2, while treatment with the AKT inhibitor MK2206 or knockout of CXCR1 or CXCR2 (Supplementary Fig. S2C, D) in HGC-27 cells reduced the nuclear expression of HK2 (Fig. 3b, c). Consistent results were observed in MGC-803 cells (Supplementary Fig. S3A); these data suggest that IL-8 and AKT are crucial for HK2 nuclear localization in GC cells.

SDS-PAGE$^{Phos-tag}$ analyses indicated that phosphorylated HK2 was only detectable in the nucleus of GC cells, whereas both phosphorylated and nonphosphorylated HK2 were detectable in the cytoplasm (Fig. 3d, Supplementary Fig. S3B). Therefore, HK2 phosphorylation is required for HK2 nuclear localization. Immunofluorescence assay confirmed that the proportion of nuclear HK2 was increased in the present of GCMSC-CM (Fig. 3e). To explore the mechanism of phosphorylated HK2 into the nucleus, we performed a Co-IP assay to identify the proteins that interact with HK2. The results showed that HK2 bound to HIF-1α in HGC-27 and MGC-803 cells (Fig. 3f), suggesting that HK2 nuclear translocation forms transcription complexes with HIF-1α, which might play a regulatory role in gene transcription. To further explore the effect of HK2 on HIF-1α transcriptional activity, we conducted EMSA and ChIP-qPCR assays. The results showed that GCMSC-CM significantly increased the occupation frequency of HIF-1α on the promoters of PD-L1 with known HIF-1α-binding motif. (Fig. 3g, h). HK2 silencing significantly reduced the levels of HIF-1α nuclear protein transcriptional activity in HGC-27 cells. In contrast, GCMSC-CM-treated GC cells had significantly increased transcriptional activity of HIF-1α, which was reversed by anti-IL-8 or AKT inhibitor MK2206 (Fig. 3i, j). Similar results were also observed in MGC-803 cells (Supplementary Fig. S3C). Taken together, our results demonstrated that GCMSC-derived IL-8 and AKT-mediated phosphorylation promotes HK2 nuclear localization and that phosphorylated-HK2 promotes the transcription of *PD-L1* by binding to HIF-1α in GC cells.

GCMSC-CM promotes GC cell proliferation via PD-L1 under serum deprivation and hypoxia

Cell-intrinsic PD-L1 might originate from intracellular sources such as the cytoplasm and nucleus, and could be elicited by surface PD-L1–PD-1 engagement, but could be PD-1 independent, despite that we have previously demonstrated that GCMSC-derived IL-8 upregulates PD-L1 expression (Fig. 4a). TCGA analysis of STAD was conducted and the data showed a significant positive correlation between *PD-L1* and *HK2* expression (Fig. 4b). We further observed that HK2 knockdown abolished the GCMSC-CM-mediated upregulation of PD-L1 (Fig. 4c). However, whether GCMSC affected cell-intrinsic PD-L1 leading to immunotherapy resistance through a PD-1-dependent mechanism is unknown. Here, we sought to explore the role of PD-L1 on GC cell proliferation in serum deprivation and hypoxia, which simulate the tumor microenvironment. We found that, under serum deprivation and hypoxia, PD-L1 overexpression significantly promoted GC cell proliferation in a time-dependent manner (Fig. 4d, e). Furthermore, key glycolytic enzymes were found to be correlated with cell-intrinsic PD-L1 expression under these conditions (Fig. 4f).

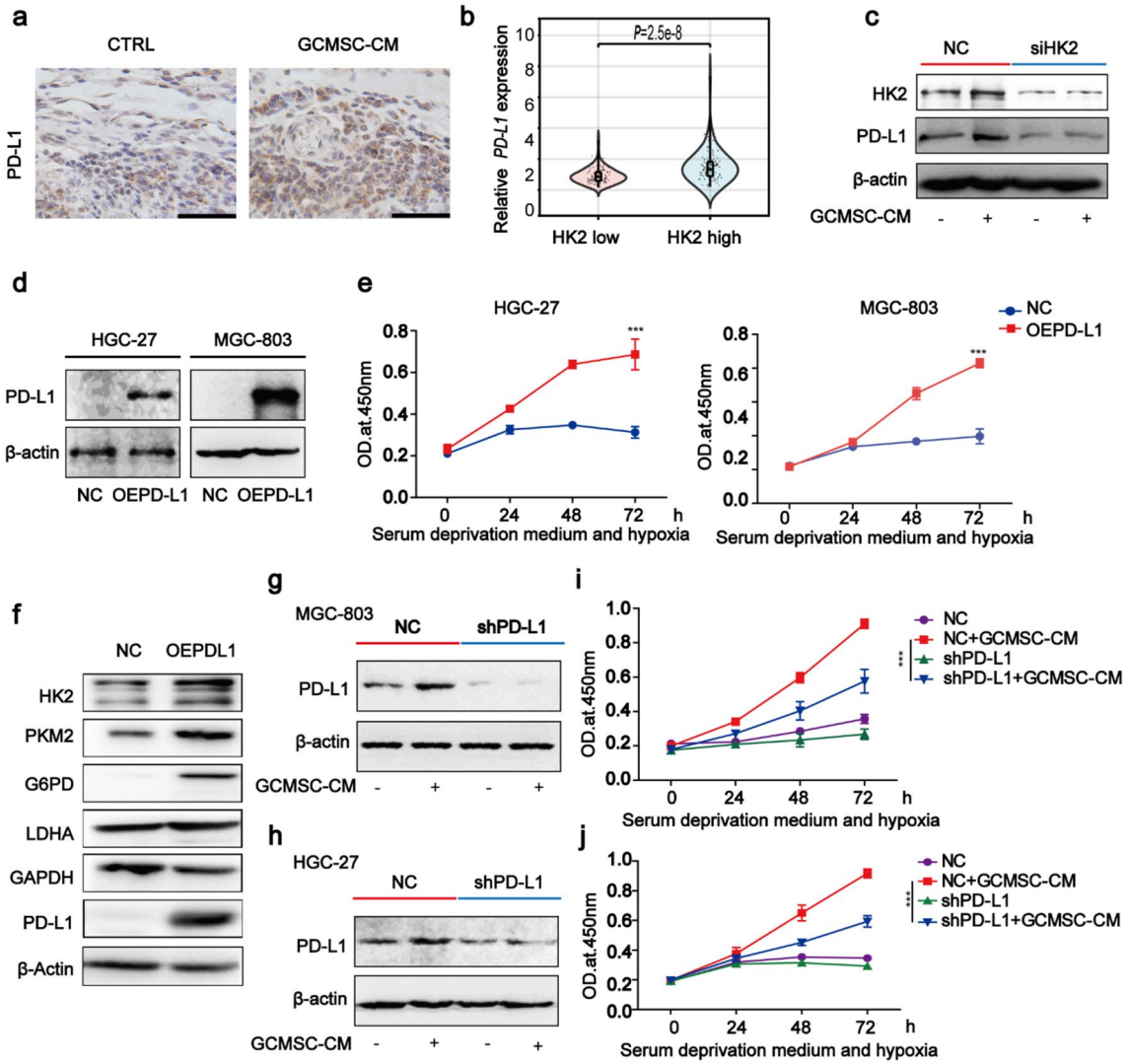

Fig. 4 GCMSC-CM promotes gastric cancer cell proliferation via PD-L1 under serum deprivation and hypoxia. **a** IHC staining of PD-L1 in xenograft tumor tissue samples from NPG^{CD34+} mice (scale bar: 50 μm). **b** PD-L1 mRNA levels in GC tissue samples with low ($n=187$) or high ($n=188$) HK2 expression were obtained from the TCGA database. **c** Immunoblot assays in HGC-27 cells that received HK2 silencing with or without GCMSC-CM treatment. **d** PD-L1 protein expression in HGC-27 or MGC-803 cells overexpressing PD-L1 or negative control. **e** The viability of wild type and OEPD-L1 of HGC-27 or MGC-803 cells was continuously observed within 72 h. **f** Immunoblot assays in MGC-803 cells under serum deprivation and hypoxia condition. **g**, **h** Immunoblot assays for PD-L1 after treatment with shRNA targeting negative control or PD-L1. **i**, **j** The viability of WT and PD-L1 KD MGC-803 or HGC-27 cells was continuously observed for 72 h. Data are expressed as the mean ± SEM. ***$P<0.001$. $n=3$. *WT* wild type. *OE* overexpression; *NC* negative control

To further investigate whether GCMSC-CM affects tumor cell proliferation through PD-L1, we performed a cell proliferation assay in PD-L1-silenced GC cells under serum deprivation and hypoxia condition (Fig. 4g, h). We found that GCMSC-CM treatment significantly promoted GC cell proliferation compared to control, while PD-L1 silencing partially but significantly attenuated GCMSC-CM-induced cell proliferation under serum deprivation and hypoxia (Fig. 4i, j), Together, these data suggest that GCMSC-CM promotes GC cell proliferation, at least partially, through PD-L1.

Blocking GCMSC-CM-derived IL-8/CXCR2 pathway restores the antitumor capacity of PD-1 antibody

To investigate whether blocking GCMSC-derived IL-8/CXCR2 pathway could restore the antitumor efficacy of PD-1 antibody, we inoculated NCG^{PBMC} mice with CXCR1/2-wild-type or CXCR1/2-knockout HGC-27 cells (Fig. 5a). Compared to the wild-type group, the depletion of CXCR1/2 in GC cells completely reversed GCMSC-CM-induced tumor growth and restored the antitumor effect of

PD-1 antibody that was suppressed by GCMSC-CM in mice (Fig. 5b, c). CXCR1/2 depletion also significantly further enhanced the effect of PD-1 antibody on the proportion of $CD8^+$ T cells in tumor tissue (Fig. 5d). In addition, CXCR1/2-knockout effectively reduced lactate level (Fig. 5e) and resulted in a decrease in the protein levels of HK2, PD-L1, and Ki67 in tumor tissue (Supplementary Fig. S4). Immunohistochemical staining showed that CXCR1/2 depletion effectively increased protein expression of IFN-γ and GZMB in tumor tissue (Fig. 5f). Correspondingly, the combination therapy of IL-8 neutralizing antibody or CXCR2 receptor antagonist demonstrated in vivo anti-PD-1 efficacy restoring in NCG^{PBMC} humanized mouse model (Fig. 5g, h), suggesting that neutralizing IL-8 or inhibiting binding to the CXCR2 receptor could reverse the antitumor capacity of anti-PD-1 antibody to a certain extent in the presence of GCMSC-CM. Taken together, these results indicated that GCMSC-derived IL-8 signaling was essential for GCMSC-CM-mediated attenuation of antitumor immunity. Blocking GCMSC-derived IL-8 signaling by CXCR1/2 depletion could effectively maintain the antitumor effect of anti-PD-1 antibody, thereby inhibiting tumor growth.

High serum IL-8 levels are associated with worse clinical outcomes of patients treated with PD-1 antibody

Then, we aimed to investigate the relationship between serum IL-8 level and the efficacy of PD-1 antibody therapy in 39 GC patients who received combination treatment with chemotherapy (Supplementary Data Table 1). Patients were stratified into two groups based on the median serum IL-8 level (26.6 pg/mL). We observed the patients with elevated serum IL-8 level was dramatically associated with a lower objective response rate (ORR) (Fig. 6a, b). Meanwhile, patients with partial response (PR) were observed to have lower serum IL-8 level after one course of immunotherapy plus chemotherapy (Fig. 6c). Here, we reported two patients with advanced gastric adenocarcinoma who had previously failed in the chemotherapy alone, but later showed a remarkable different clinical response after treatment with an anti-PD-1 antibody in combination with chemotherapy (Fig. 6d). A higher expression of IL-8 in GC tissue was significantly associated with worse overall survival (OS) in patients. In patients with lower MSCs gene set expression, no significant correlation was observed between IL-8 expression and the overall survival in patients (Fig. 6e). In addition, we found no significant correlation between CXCL8 mRNA level and the prognosis of patients with stage III or IV gastric cancer, with the majority population administered anti-PD-1-based immunotherapy combined with chemotherapy (Supplementary Fig. S5A). However, in GC patients with enriched MSCs gene set expression, high IL-8 expression was significantly associated with worse OS (Fig. 6f). Taken together, our findings indicate that GCMSC is closely related to the prognosis of receiving PD-1 antibody therapy in the $CXCL8^{high}$ group of GC patients.

Discussion

PD-1/PD-L1 antibodies provide new hope for tumor patients. Recent long-term follow-up results showed that nivolumab (anti-PD-1) plus chemotherapy demonstrated improvement in overall survival versus chemotherapy alone for advanced gastro-oesophageal adenocarcinoma [16]. For the foreseeable future, nivolumab plus chemotherapy will be an important treatment strategy for unresectable GC patients. However, there are still obstacles to be overcome in immunosuppressive therapy. Here, we raise a presumption that the "IL-8−CXCR2–HK2–HIF1α–PD-L1" dual inhibition pathway could play a critical role in antitumor immunity (Fig. 7).

One of the most significant characteristics of the tumor microenvironment (TME) is hypoxia. HIF-1α is initially identified as an important factor in response to hypoxic conditions, and HIF-1α and c-Myc are two critical transcriptional factors that maintain high glycolytic activity in cancer cells [17], resulting in upregulating lactate production through multiple mechanisms, including but not limited to promoting the expression of glycolysis key enzymes hexokinase 2 (HK2) and lactate dehydrogenase (LDH) and suppressing pyruvate kinase 2 (PKM2) activity to limit pyruvate into mitochondrial metabolism [18]. The classical physiological roles of these proteins are well established. However, the non-canonical function for metabolic enzymes have aroused the interest of researchers [19, 20]. The biochemical discovery of HK2–HIF-1α interaction was inspired by dimeric/monomeric PKM2-regulated HIF-1α activity via forming a complex with HIF-1α.

In the tumor microenvironment, elevated lactate suppresses the antitumor activity of T cells by increasing the accumulation of H^+ and maintaining low pH in the TME. Neutralization of acidic TME and proton-pump inhibitors enable reversing the suppression of antitumor immunity and improve immunotherapy [21]. Mechanistically, lactic acidosis can impair the IFN-γ production of CTLs. Furthermore, lactate can modulate $CD4^+$ T cell polarization and reduce the percentage of the antitumoral T-helper 1 subset by inducing SIRT1-mediated deacetylation/degradation of T-bet transcription factor. Additionally, MCT1-mediated lactate influx and intracellular lactate metabolism are important for tumor-infiltrating Treg cells to sustain their suppressive activity [22]. In addition, a novel post-transcriptional modification driven by lactic acid, lactylation, plays a vital role in cancer, inflammation, and regeneration [23].

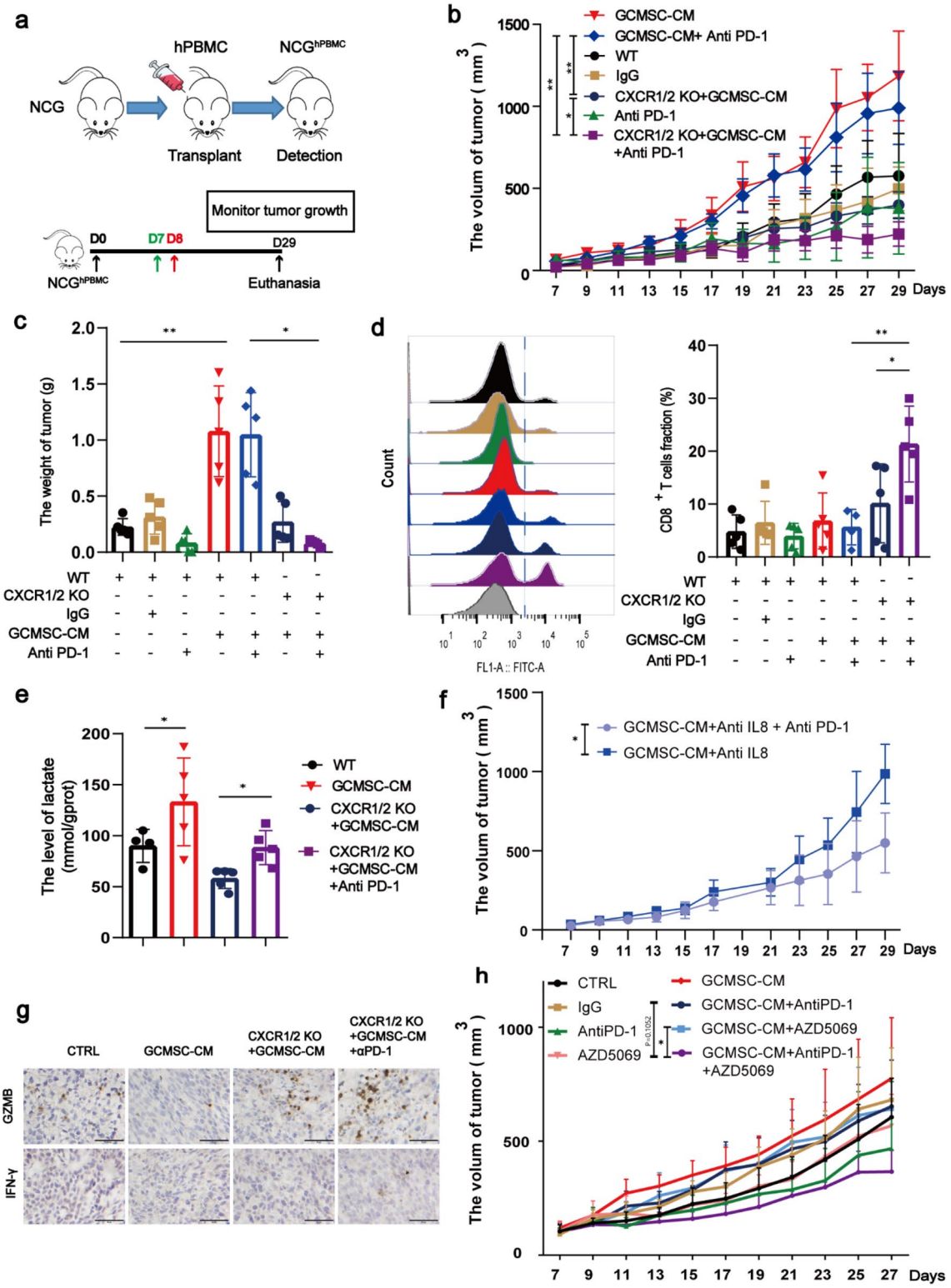

According to NPG^{CD34+} humanized mouse model, CD8^{+} T cells were recruited around the tumor tissue, but failed to infiltrate into the tumor tissue in the GCMSC-CM treatment group. We hypothesized that other factors might decrease the antitumor ability of T cells. Glycolysis reprogramming would be an important reason for this phenomenon based on our previously study [15]. Therefore, we detected the lactate level in the GCMSC-CM treatment group or GC tissues. Interestingly, in the presence of GCMSC-CM, lactate levels were significantly elevated accompanied by increased

◂**Fig. 5** Blocking GCMSC-CM-derived IL-8 signaling on GC cells restores the antitumor capacity of PD-1 antibody. **a** Schematic diagram of HGC-27 tumors in the NCG^{PBMC} model. "Green" arrows show "administered GCMSC-CM (200uL) via subcutaneous injection peritumoral", "red" arrows show "administered pembrolizumab (10 mg/kg) via intraperitoneal injection". Mice were inoculated with wild type or CXCR1/2 knockout on day 0 (back, s.c.). Mice were administered GCMSC-CM every other day starting day 7 (green, s.c.). Mice were administered five doses of Keytruda every 3 days starting day 8 (red, 10 mg/kg i.p.). **b** Tumor volumes were measured every 2 days. **c** Tumors were collected and weighted. **d** Flow cytometry analysis for $CD8^+$ cells infiltrating into tumor tissues. **e** Lactate levels in mouse tumor tissue samples. **f** HGC-27 tumors in NCG^{PBMC} mice model were administered with or without IL-8 neutralizing antibody every 2 days before GCMSC-CM treatment starting day 7, and tumor volumes were measured every 2 days. **g** IHC staining of IFN-γ and GZMB in HGC-27 xenograft tumor tissue samples. **h** MGC-803 tumors in NCG^{PBMC} mice model were administered with or without CXCR2 receptor inhibitor AZD5069 every 2 days before GCMSC-CM treatment starting day 7, and tumor volumes were measured every 2 days. Data are expressed as the mean ± SEM. $^*P < 0.05$, $^{**}P < 0.01$, $^{***}P < 0.001$; $n = 6$. *WT* wild type; *KO* knockout

HK2 protein expression. Whether it the increase in the total amount of HK2 or the increased activity that leads to excess lactate production remains to be further investigated.

However, the reason for the lack of increase in the proportion of $CD3^+CD8^+$ cells in the anti-PD-1 treatment alone group remains to be further investigated. Perhaps, as Haofei Liu et al. have suggested, anti-PD-1 administration alone could partially alleviate $CD8^+$ T cell exhaustion in vivo [24]. On the other hand, we believe that the quantity of infiltrating immune cells is a prerequisite for the effectiveness of anti-PD-1 therapy. A promising approach to enhancing the efficacy of anti-PD-1 treatment is to block the inhibitory effect driven by GCMSCs.

In our previous study, we have observed the proportion of Treg cells increased in GCMSC-CM-pretreated PBMCs [25]. Therefore, we performed flow cytometry to detect the surface markers of Treg cells in $CD34^+$ humanized mouse model tumor. The results revealed a significant upregulation of Treg cell proportion in the GCMSC-CM group, suggesting that the immunosuppressive effect of GCMSCs partly depends on inducing the differentiation of Treg cells.

Furthermore, flow cytometry was limited in its ability to differentiate immune cell infiltration from the peritumoral or intratumoral areas. Therefore, systemically characterizing T cells would be more effective in investigating their anatomic distribution in tumors.

Tumor cells can reprogram intratumoral MSCs through multiple mechanisms, including enhancing proliferative and metastatic abilities, promoting cytokine production, and reprogramming metabolism [13], and these educated MSCs also provide feedback into tumor cells [12, 26, 27]. In the GC microenvironment, GCMSCs produce excess proinflammatory cytokines, such as IL-8, IL-6, and hepatocyte growth factor [11, 28]. At the same time, we noted in two clinical retrospective studies that tumor-associated or serum IL-8 inhibits antitumor immunity, and that patient serum IL-8 is related to reduced clinical benefit of immune-checkpoint inhibitors [9, 10]; however, they did not cover stomach cancer. Therefore, we focused on whether GCMSCs-derived IL-8 mediate immunosuppression in anti-PD-1 therapy. What is more, whether IL-8 high level is associated with poor prognosis in GC patients remains to be explored. However, it has been reported that high pretherapeutical serum IL-8 level in GC patients was associated with poor response to platinum-based therapy [29]. A population of gastric cancer patients who had received at least one chemotherapy showed no significant correlation between IL-8 expression and the overall survival (Supplementary Fig. S5B). Therefore, the relationship between serum IL-8 and combined chemotherapy should be further explored in a large number of clinical samples.

Infiltration of immune cells in solid tumors also affects the therapeutic effect of PD-1 antibody. T cells in tumors, especially in responsive patients, are replenished with fresh, non-depleted replacement cells from the sites outside the tumor, suggesting that these patients have a continuously active tumor immunity cycle that accelerates the clinical response [30]. In the NPG^{CD34+} humanized mouse model, we observed that $CD8^+$ T cells were recruited around the tumor tissue, but failed to infiltrate into tumor tissue in the GCMSC-CM treatment group, suggesting that we should pay more attention to the function and distribution of tumor-infiltrating lymphocytes (TILs). However, for NCG^{PBMC} humanized mouse model, $CD8^+$ T cell subpopulation proportion upregulation was not observed with GCMSC-CM. Perhaps, the difference comes from animal model, as no continuous lymphocyte replenishment is derived from hematopoietic stem cells.

Due to the lack of IL-8 homologs in the mouse genome and the limited types of murine GC cell lines that differ from human GC cells, it has been difficult to study the mechanism of IL-8 related immunotherapy resistance in preclinical models [31]. To solve these problems, we deployed human hematopoietic stem cells and human PBMCs to construct humanized immune system-engrafted mouse models to take advantage of both animal models. Together with human GC cell lines and GCMSCs isolated from human GC tissue, the mouse models deployed in this study are ideal for studying human tumor biology.

Moonlighting, the ability of a protein to perform two or more unrelated functions, has been demonstrated for many metabolic enzymes [32]. The non-canonical function of metabolic enzymes such as PKM2 and FBP1 can act as protein phosphatases to regulate gene transcription [33, 34]. The canonical metabolic function of HK2 is to bind to mitochondrial membrane in glycolysis occurs in the cytoplasm. Also, HK2 activity and localization are dynamically regulated by

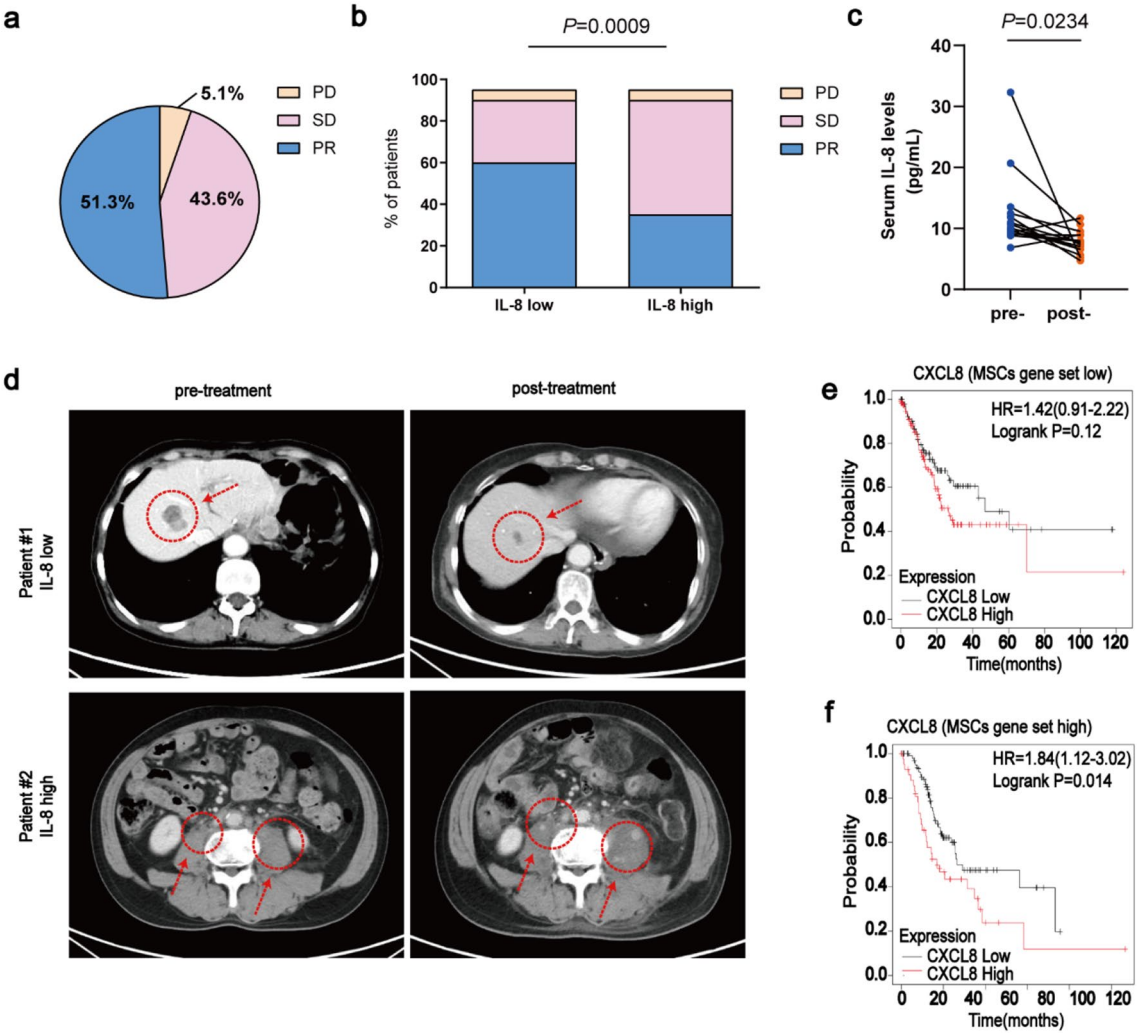

Fig. 6 The association of serum IL-8 levels with clinical outcomes in GC patients. **a** Clinical outcome assessments of the cohort of 39 unresectable GC patients treated with anti-PD-1-based immunotherapy combined with chemotherapy. PR (20/39), SD (17/39), PD (2/39). Best change from baseline in the tumor burden per patient referring to the RECIST guidelines. **b** Correlation of serum IL-8 levels and patient responses to PD-1 antibody treatment in gastric cancer. **c** Serum IL-8 concentration in paired samples after one course of treatment. **d** Two representative patients with unresectable GC who were chemorefractory and then treated with PD-1 blockade combined with chemotherapy. **e**, **f** Kaplan–Meier analysis of the correlation of IL-8 mRNA expression with the overall survival of gastric cancer patients, gastric cancer patients with decreased mesenchymal stem cells (**e**), or with enriched mesenchymal stem cells (**f**). The data were obtained from the Kaplan–Meier plot http://kmplot.com/. *PR* partial response; *SD* stable disease; *PD* progressive disease, *MSCs* mesenchymal stem cells

its phosphorylation. Geethu Emily Thomas et al. proposed that HK2 nuclear translocation occurs independently of its kinase activity [19]. AKT phosphorylates HK2 at Thr 473 to enable its docking to mitochondria [35], while phosphorylation of HK2 at T473 promotes tumorigenesis and metastasis in colon cancer cells [36]. Therefore, we hypothesized that HK2 dissociates from mitochondria and is involved in tumor progression as a protein kinase. Our findings demonstrate that phosphorylation is essential for HK2 nuclear localization, and knockdown of HK2 or inhibition of AKT phosphorylation reduces the transcriptional activity of HIF-1α. However, the evidence for the interaction between HK2 and HIF-1α is not strong enough, and it is unclear whether they bind in the cytoplasm or nucleus, whether HK2–HIF-1α complex formation inhibits HIF-1α degradation in the cytoplasm or increases HIF-1α transcriptional activity in the nucleus directly, or whether both exist simultaneously. To address these questions, we propose employing phosphorylated proteomics to identify the phosphorylation site(s) of HK2 and develop site-specific antibodies or site-mutated proteins to confirm that HIF-1α promotes PD-L1 transcription in a p-HK2-dependent manner in the following study.

Prediction of patient response is important in anti-PD-1 therapy. PD-L1 score [37], microsatellite stability, and tumor

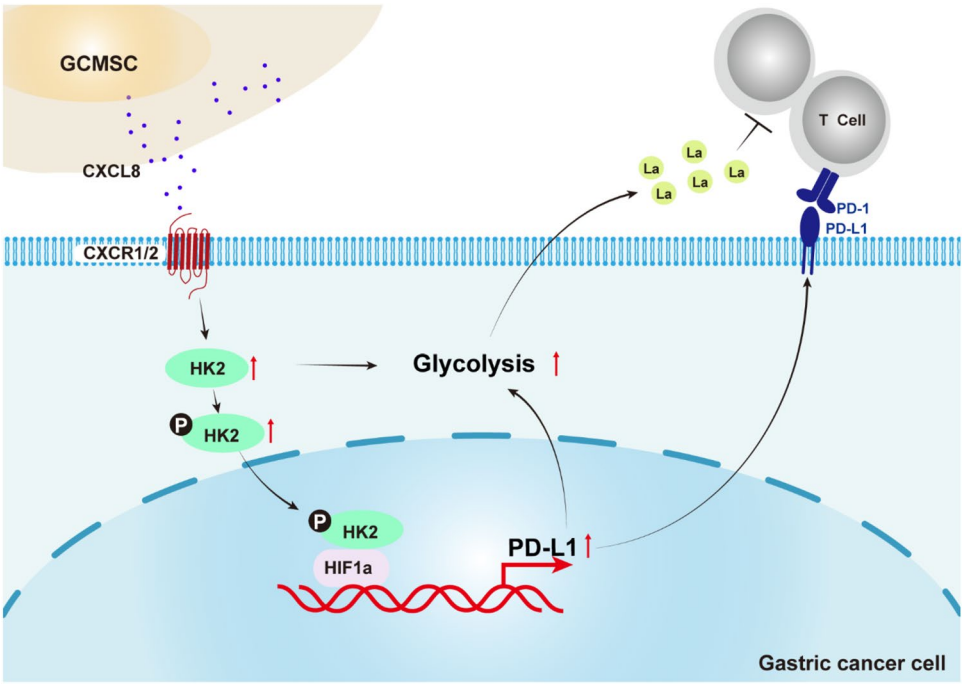

Fig. 7 Schematic diagram. IL-8 derived from GCMSCs inhibits antitumor immunity by upregulating PD-L1 expression and promoting lactate production in gastric cancer cells. GCMSCs promote gastric tumor growth while attenuating antitumor efficacy of PD-1 antibody. Blocking IL-8 signaling may improve the antitumor efficacy of anti-PD-1 therapy for gastric cancer treatment through suppressing gastric tumor growth, reducing lactate production, and suppressing PD-L1 expression

mutation burden have been implicated in patient response to anti-PD-1 therapy [38]. There is still a lack of guidance for GC patient selection. In this study, we observed that high serum and tumoral IL-8 levels were associated with worse clinical outcomes of patients treated with PD-1 antibody. However, patients suffering from advanced GC are rarely treated with anti-PD-1 alone; therefore, the patient serum sample we collected to assay the clinical outcome was treated with anti-PD-1-based immunotherapy combined with chemotherapy. In summary, our data suggest that IL-8 may serve as a potential predictive factor for patient response to anti-PD-1 therapy.

Supplementary Information The online version contains supplementary material available at https://doi.org/10.1007/s10120-023-01405-1.

Acknowledgements The authors thank AstraZeneca (China) Co. Ltd., for providing AZD5069 drug during the research.

Author contributions CH and BC: conceptualization, methodology, validation, data curation, formal analysis, writing—original draft preparation. YYZ, QQW, LS, and QZG: validation, formal analysis. ZHC, CLZ, DQW, JX, XW: resources. MW, XZ and WRX: conceptualization. WZ and BS: writing—review and editing, supervision, funding acquisition.

Funding This work was supported by the National Natural Science Foundation of China No. 81972313 (WZ), No. 81972822 (BS), No. 82203547 (LS), the Bethune Charitable Foundation No. G-X-2019-0101-12 (BS).

Data availability The data supporting the findings of this study are available from the corresponding author upon reasonable request, e-mail: zhuwei@ujs.edu.cn.

Declarations

Conflict of interest The authors declare no potential conflicts of interest.

Ethical approval This study involves human subjects, and all samples were obtained following individual informed consent and ethical approval by the Ethics Committee of the Affiliated Cancer Hospital of Nanjing Medical University ID#: 2021ke-010. The subjects gave informed consent to participate in the study before taking part. The animal study was approved by the Ethics Committee of Jiangsu University. All procedures were conducted following the guidelines of the National Institute of Health regarding the care and use of laboratory animals (NIH Publication No. 8023, revised 1978) ID#: UJS-IACUC-AP-2022022812.

References

1. Janjigian YY, Bendell J, Calvo E, Kim JW, Ascierto PA, Sharma P, et al. CheckMate-032 study: efficacy and safety of nivolumab and nivolumab plus ipilimumab in patients with metastatic esophagogastric cancer. J Clin Oncol. 2018;36(28):2836–44. https://doi.org/10.1200/JCO.2017.76.6212.
2. Shitara K, Ozguroglu M, Bang YJ, Di Bartolomeo M, Mandala M, Ryu MH, et al. Pembrolizumab versus paclitaxel for previously treated, advanced gastric or gastro-oesophageal junction cancer (KEYNOTE-061): a randomised, open-label, controlled, phase 3 trial. Lancet. 2018;392(10142):123–33. https://doi.org/10.1016/S0140-6736(18)31257-1.
3. Nanda R, Chow LQ, Dees EC, Berger R, Gupta S, Geva R, et al. Pembrolizumab in patients with advanced triple-negative breast cancer: phase Ib KEYNOTE-012 study. J Clin Oncol. 2016;34(21):2460–7. https://doi.org/10.1200/JCO.2015.64.8931.

4. Wieser V, Adolph TE, Enrich B, Kuliopulos A, Kaser A, Tilg H, et al. Reversal of murine alcoholic steatohepatitis by pepducin-based functional blockade of interleukin-8 receptors. Gut. 2017;66(5):930–8. https://doi.org/10.1136/gutjnl-2015-310344.
5. Eruslanov EB, Bhojnagarwala PS, Quatromoni JG, Stephen TL, Ranganathan A, Deshpande C, et al. Tumor-associated neutrophils stimulate T cell responses in early-stage human lung cancer. J Clin Investig. 2014;124(12):5466–80. https://doi.org/10.1172/JCI77053.
6. Liu Y, Zhang Y, Wang S, Dong QZ, Shen Z, Wang W, et al. Prospero-related homeobox 1 drives angiogenesis of hepatocellular carcinoma through selectively activating interleukin-8 expression. Hepatology. 2017;66(6):1894–909. https://doi.org/10.1002/hep.29337.
7. Shang A, Gu C, Zhou C, Yang Y, Chen C, Zeng B, et al. Exosomal KRAS mutation promotes the formation of tumor-associated neutrophil extracellular traps and causes deterioration of colorectal cancer by inducing IL-8 expression. Cell Commun Signal. 2020;18(1):52. https://doi.org/10.1186/s12964-020-0517-1.
8. Siu MKY, Jiang YX, Wang JJ, Leung THY, Ngu SF, Cheung ANY, et al. PDK1 promotes ovarian cancer metastasis by modulating tumor-mesothelial adhesion, invasion, and angiogenesis via alpha5beta1 integrin and JNK/IL-8 signaling. Oncogenesis. 2020;9(2):24. https://doi.org/10.1038/s41389-020-0209-0.
9. Schalper KA, Carleton M, Zhou M, Chen T, Feng Y, Huang SP, et al. Elevated serum interleukin-8 is associated with enhanced intratumor neutrophils and reduced clinical benefit of immune-checkpoint inhibitors. Nat Med. 2020;26(5):688–92. https://doi.org/10.1038/s41591-020-0856-x.
10. Yuen KC, Liu LF, Gupta V, Madireddi S, Keerthivasan S, Li C, et al. High systemic and tumor-associated IL-8 correlates with reduced clinical benefit of PD-L1 blockade. Nat Med. 2020;26(5):693–8. https://doi.org/10.1038/s41591-020-0860-1.
11. Sun L, Wang Q, Chen B, Zhao Y, Shen B, Wang H, et al. Gastric cancer mesenchymal stem cells derived IL-8 induces PD-L1 expression in gastric cancer cells via STAT3/mTOR-c-Myc signal axis. Cell Death Dis. 2018;9(9):928. https://doi.org/10.1038/s41419-018-0988-9.
12. Wang Q, Huang C, Ding Y, Wen S, Wang X, Guo S, et al. Inhibition of CCCTC Binding Factor-Programmed Cell Death Ligand 1 Axis Suppresses Emergence of Chemoresistance Induced by Gastric Cancer-Derived Mesenchymal Stem Cells. Front Immunol. 2022;13:884373. https://doi.org/10.3389/fimmu.2022.884373.
13. Donnelly JM, Engevik AC, Engevik M, Schumacher MA, Xiao C, Yang L, et al. Gastritis promotes an activated bone marrow-derived mesenchymal stem cell with a phenotype reminiscent of a cancer-promoting cell. Dig Dis Sci. 2014;59(3):569–82. https://doi.org/10.1007/s10620-013-2927-z.
14. Sun L, Wang Q, Chen B, Zhao Y, Shen B, Wang X, et al. Human gastric cancer mesenchymal stem cell-derived IL15 contributes to tumor cell epithelial-mesenchymal transition via upregulation tregs ratio and PD-1 expression in CD4(+)T cell. Stem Cells Dev. 2018;27(17):1203–14. https://doi.org/10.1089/scd.2018.0043.
15. Chen B, Cai T, Huang C, Zang X, Sun L, Guo S, et al. G6PD-NF-kappaB-HGF signal in gastric cancer-associated mesenchymal stem cells promotes the proliferation and metastasis of gastric cancer cells by upregulating the expression of HK2. Front Oncol. 2021;11:648706. https://doi.org/10.3389/fonc.2021.648706.
16. Shitara K, Ajani JA, Moehler M, Garrido M, Gallardo C, Shen L, et al. Nivolumab plus chemotherapy or ipilimumab in gastro-oesophageal cancer. Nature. 2022;603(7903):942–8. https://doi.org/10.1038/s41586-022-04508-4.
17. Gordan JD, Thompson CB, Simon MC. HIF and c-Myc: sibling rivals for control of cancer cell metabolism and proliferation. Cancer Cell. 2007;12(2):108–13. https://doi.org/10.1016/j.ccr.2007.07.006.
18. Wang ZH, Peng WB, Zhang P, Yang XP, Zhou Q. Lactate in the tumour microenvironment: From immune modulation to therapy. EBioMedicine. 2021;73:103627. https://doi.org/10.1016/j.ebiom.2021.103627.
19. Thomas GE, Egan G, Garcia-Prat L, Botham A, Voisin V, Patel PS, et al. The metabolic enzyme hexokinase 2 localizes to the nucleus in AML and normal haematopoietic stem and progenitor cells to maintain stemness. Nat Cell Biol. 2022;24(6):872–84. https://doi.org/10.1038/s41556-022-00925-9.
20. Palsson-McDermott EM, Curtis AM, Goel G, Lauterbach MA, Sheedy FJ, Gleeson LE, et al. Pyruvate kinase M2 regulates Hif-1alpha activity and IL-1beta induction and is a critical determinant of the warburg effect in LPS-activated macrophages. Cell Metab. 2015;21(1):65–80. https://doi.org/10.1016/j.cmet.2014.12.005.
21. Ippolito L, Morandi A, Giannoni E, Chiarugi P. Lactate: a metabolic driver in the tumour landscape. Trends Biochem Sci. 2019;44(2):153–66. https://doi.org/10.1016/j.tibs.2018.10.011.
22. Watson MJ, Vignali PDA, Mullett SJ, Overacre-Delgoffe AE, Peralta RM, Grebinoski S, et al. Metabolic support of tumour-infiltrating regulatory T cells by lactic acid. Nature. 2021;591(7851):645–51. https://doi.org/10.1038/s41586-020-03045-2.
23. Xin Q, Wang H, Li Q, Liu S, Qu K, Liu C, et al. Lactylation: a passing fad or the future of posttranslational modification. Inflammation. 2022;45(4):1419–29. https://doi.org/10.1007/s10753-022-01637-w.
24. Liu H, Zhao Q, Tan L, Wu X, Huang R, Zuo Y, et al. Neutralizing IL-8 potentiates immune checkpoint blockade efficacy for glioma. Cancer Cell. 2023;41(4):693-710 e8. https://doi.org/10.1016/j.ccell.2023.03.004.
25. Wang M, Chen B, Sun XX, Zhao XD, Zhao YY, Sun L, et al. Gastric cancer tissue-derived mesenchymal stem cells impact peripheral blood mononuclear cells via disruption of Treg/Th17 balance to promote gastric cancer progression. Exp Cell Res. 2017;361(1):19–29. https://doi.org/10.1016/j.yexcr.2017.09.036.
26. Wang M, Zhao X, Qiu R, Gong Z, Huang F, Yu W, et al. Lymph node metastasis-derived gastric cancer cells educate bone marrow-derived mesenchymal stem cells via YAP signaling activation by exosomal Wnt5a. Oncogene. 2021;40(12):2296–308. https://doi.org/10.1038/s41388-021-01722-8.
27. Gao QZ, Cui LJ, Huang C, Zhou CL, Chen B, Wang QQ, et al. Gastric cancer-derived exosomes induce PD-L1 expression on human bone marrow mesenchymal stem cells through the AKT-c-Myc signal axis. All Life. 2022;15(1):442–51. https://doi.org/10.1080/26895293.2022.2058098.
28. Sun L, Huang C, Zhu M, Guo S, Gao Q, Wang Q, et al. Gastric cancer mesenchymal stem cells regulate PD-L1–CTCF enhancing cancer stem cell-like properties and tumorigenesis. Theranostics. 2020;10(26):11950–62. https://doi.org/10.7150/thno.49717.
29. Zhai J, Shen J, Xie G, Wu J, He M, Gao L, et al. Cancer-associated fibroblasts-derived IL-8 mediates resistance to cisplatin in human gastric cancer. Cancer Lett. 2019;454:37–43. https://doi.org/10.1016/j.canlet.2019.04.002.
30. Wu TD, Madireddi S, de Almeida PE, Banchereau R, Chen YJ, Chitre AS, et al. Peripheral T cell expansion predicts tumour infiltration and clinical response. Nature. 2020;579(7798):274–8. https://doi.org/10.1038/s41586-020-2056-8.
31. Lee YS, Choi I, Ning Y, Kim NY, Khatchadourian V, Yang D, et al. Interleukin-8 and its receptor CXCR2 in the tumour microenvironment promote colon cancer growth, progression and metastasis. Br J Cancer. 2012;106(11):1833–41. https://doi.org/10.1038/bjc.2012.177.
32. Jeffery CJ. Moonlighting proteins. Trends Biochem Sci. 1999;24(1):8–11. https://doi.org/10.1016/s0968-0004(98)01335-8.

33. Wang Z, Li M, Jiang H, Luo S, Shao F, Xia Y, et al. Fructose-1,6-bisphosphatase 1 functions as a protein phosphatase to dephosphorylate histone H3 and suppresses PPARalpha-regulated gene transcription and tumour growth. Nat Cell Biol. 2022;24(11):1655–65. https://doi.org/10.1038/s41556-022-01009-4.
34. Yang W, Xia Y, Hawke D, Li X, Liang J, Xing D, et al. PKM2 phosphorylates histone H3 and promotes gene transcription and tumorigenesis. Cell. 2012;150(4):685–96. https://doi.org/10.1016/j.cell.2012.07.018.
35. Roberts DJ, Tan-Sah VP, Smith JM, Miyamoto S. Akt phosphorylates HK-II at Thr-473 and increases mitochondrial HK-II association to protect cardiomyocytes. J Biol Chem. 2013;288(33):23798–806. https://doi.org/10.1074/jbc.M113.482026.
36. Li H, Lu S, Chen Y, Zheng L, Chen L, Ding H, et al. AKT2 phosphorylation of hexokinase 2 at T473 promotes tumorigenesis and metastasis in colon cancer cells via NF-kappaB, HIF1alpha, MMP2, and MMP9 upregulation. Cell Signal. 2019;58:99–110. https://doi.org/10.1016/j.cellsig.2019.03.011.
37. Chen G, Huang AC, Zhang W, Zhang G, Wu M, Xu W, et al. Exosomal PD-L1 contributes to immunosuppression and is associated with anti-PD-1 response. Nature. 2018;560(7718):382–6. https://doi.org/10.1038/s41586-018-0392-8.
38. Le DT, Durham JN, Smith KN, Wang H, Bartlett BR, Aulakh LK, et al. Mismatch repair deficiency predicts response of solid tumors to PD-1 blockade. Science. 2017;357(6349):409–13. https://doi.org/10.1126/science.aan6733.